

SIMULATING PATTERNS OF UNCERTAINTY IN POST-CLASSIFICATION CHANGE DETECTION

Amy C. Powers

School of Natural Resources & Environment, University of Michigan,
Ann Arbor, MI 48104-1041 USA

Tel: +1 734-647-7341

Email: aburnick@umich.edu

1. Introduction

Detecting land-cover changes using a post-classification change analysis simply amounts to overlaying classified maps from two different dates and creating either a Boolean map of change and no change areas, or a more detailed map that identifies each possible land-cover transition. However, each land-cover map has its own patterns of misclassification. The challenge lies in determining how to quantify the manner in which the error estimates from each individual classification combine to form the error associated with change detection. This requires an understanding of the uncertainties associated with the individual land-cover-classified maps and an understanding of how these uncertainties interact over time. Thus, an important first step in assessing the accuracy associated with land-cover-change is to address the impact temporal dependencies have in creating the final error patterns present in a resulting post-classification change map.

It is often assumed that the accuracy of a change map equals the product of the accuracies of the individual land cover maps (Congalton & Green, 1999), or that one can assume temporal independence in order to model the propagation of error across a series of thematic maps (Pontius & Lippitt, 2004). Further, it is often argued that the existence of a temporal dependence between the errors of individual land-cover-classified maps can be safely ignored in most land-cover-change analyses. For example, in developing their combined locational/classification error model, Carmel & Dean (2004) argue that although the existence of temporal dependence between the errors of classified imagery can influence the uncertainty associated with their calculated measure of overall error, such dependencies are often minor and negligible in most land-cover-change studies. In contrast, recent research has found that significant differences exist between the overall change accuracy of a series of classified maps and that calculated by simply multiplying the individual accuracies of the classified maps (Liu & Zhou, 2004; Powers, 2004). This difference is primarily due to temporal interactions occurring between the individual maps. Further, recent research has also illustrated that significant temporal interactions occur between errors in time-series classified land-cover maps (Carmel, 2004; Powers, 2004). Therefore, in order to fully understand the accuracy of a change map, a greater understanding of how classification errors from different temporal maps interact and affect our ability to detect change is required. Only by comprehending how errors propagate through a change analysis over time will researchers be able to quantify and present a more thorough description of uncertainty in land cover change products.

The presented research describes the impact temporal dependencies have on the error patterns associated with change maps produced when conducting post-classification change-detection. To achieve this goal, a simulation model is developed that allows one to control both the pattern and magnitude of the classification errors associated with individual land-cover maps and level of temporal dependence between these error patterns to determine the impact increasing levels of temporal dependence have on the resulting error pattern of the land-cover-change map. Stochastic simulation is used to create both the time-series pair of land-cover maps exhibiting varying patterns of change and the time-series pair of associated land-cover maps perturbed by varying patterns of error. These maps are then analyzed in a post-classification change analysis to assess the relative performance of the error-perturbed maps in identifying and quantifying known land-cover changes. A variety of change patterns and a series of error patterns exhibiting increasing levels of temporal correlation are investigated and compared.

2. A Simulation Model of Land-Cover Change

Simulation was chosen to investigate the impact of temporal dependencies in post-classification change-detection because it allows for the definition of the spatial error patterns of the individual land-cover classifications, as well as the degree of temporal dependence between the error patterns. This complete understanding of the error patterns associated with classified land-cover maps is often not available when utilizing real-world data. Further, the use of simulation provides a controlled platform for experimentation allowing one to readily assess and compare the affect varying error or change patterns have on the resulting accuracy of the change map. There are many examples of research studies that investigated error propagation in remotely-sensed databases through the use of simulated datasets due to the ability to define and control the various error inputs and structures (Carmel & Dean, 2004; Arbia et al, 1998; Goodchild et al, 1992). Additionally, simulation also enables the generation of multiple representations of the uncertainty associated with each of the resulting error-perturbed land-cover-change maps. This permitted a more thorough analysis and comparison of the impact various patterns of error and levels of temporal dependence had on the relative performance of resulting post-classification change map.

Simulated annealing was used to produce both the time-series pair of classified land-cover maps and the time-series pair of associated error-perturbed land-cover maps. Although simulated annealing has seen limited use in research involving remotely-sensed data (Bárdossy & Samaniego, 2002; Goovaerts & Journel, 1996), it offers a great deal of flexibility in producing multiple realizations for both time-series pairs of maps. All main model components that comprise the land-cover simulation model were produced, in part, using simulated annealing. Generally, simulated annealing is a flexible simulation algorithm that requires no definition of an initial random function model (Goovaerts, 1997), but instead attempts to reproduce user-defined target statistics by modifying an initial image. Its flexibility is a direct result of the ability to define the objective function that the algorithm uses to determine which perturbations are acceptable. Objective function parameters of primary interest in this research included: 1) semivariogram models that represent the spatial continuity of the individual land-cover classes in each classified map and the spatial continuity of their associated error patterns, and 2) linear correlations between the error patterns of individual classified maps to impart temporal dependence. Since many possible solutions to the optimization algorithm exist, a series of

realizations are produced that allow one to quantify the uncertainty inherent in performing post-classification land-cover change.

2.1 Overall Model Framework

The overall land-cover change model was comprised of three main components produced through simulated annealing: 1) initial time-1 land-cover classification probability surfaces, 2) change probability surfaces, and 3) time-1 and time-2 associated error probability surfaces.

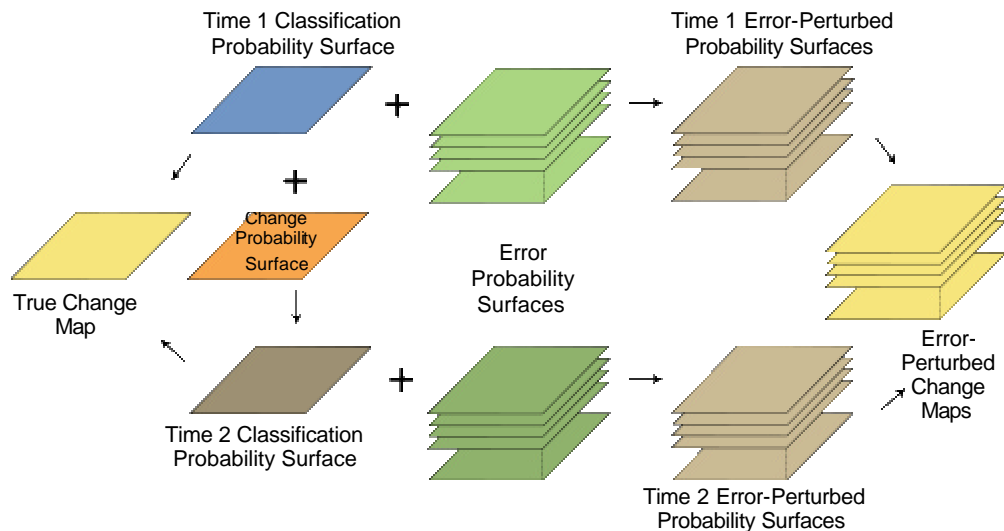


Figure 1. Diagram of the overall land-cover change simulation model used to investigate the impact of temporal dependencies on post-classification change maps.

Specifically, the flow of the overall land-cover change model can be broken down into two major components: generation of a true change map and generation of a series of error-perturbed change maps (Figure 1). The generation of the true change map involved:

- generation of the time-1 classification probability surface,
- generation of the change probability surface,
- addition of the time-1 classification probability surface and change probability surface to produce the time-2 classification probability surface,
- assignment of land-cover classes to both the time-1 and time-2 classification probability surfaces, and
- generation of the true map of land-cover change.

While the generation of the series of error-perturbed change maps involved:

- generation of a separate series of error probability surfaces for both time-1 and time-2,
- addition of the time-1 and time-2 classification probability surfaces to its associated series of error probability surfaces to produce the time-1 and time-2 error-perturbed classification probability surfaces,
- assignment of land-cover classes to both the time-1 and time-2 series of error-perturbed classification probability surfaces, and
- generation of the series of error-perturbed maps of change.

Finally, the series of error-perturbed change maps were compared to the true map of land-cover change to evaluate the relative performance of each error/change pattern combination in accurately capturing the observed true changes. Accuracy measures, such as the overall percent correctly classified (PCC) and user's accuracy of the combined change classes, were then calculated and compared for each combination.

All land-cover classifications performed in this research were constrained to only two possible land-cover classes, with classification probability cut-offs corresponding to the mean, or 50th percentile, of the initial probability distribution used to generate the probability surfaces. For all three probability surfaces generated (time-1 classification, change, and error), normal distributions were used to produce the initial random maps created during the first step of simulated annealing. Therefore, for land-cover classifications resulting from the addition of multiple independent probability surfaces (e.g. time-1 + change), the classification cut-off was determined using the theorem governing linear combinations of independent normally distributed random variables that states if X_1, X_2, \dots, X_n are mutually independent normal variables with means $\mu_1, \mu_2, \dots, \mu_n$ and variances s_1, s_2, \dots, s_n then the linear function:

$$Y = \sum_{i=1}^n a_i X_i \quad (1)$$

has normal distribution:

$$N\left(\sum_{i=1}^n a_i \mu_i, \sum_{i=1}^n a_i^2 s_i^2\right) \quad (2)$$

where a_1, a_2, \dots, a_n are real constants (Hogg & Tanis, 1993). Simulated annealing was conducted using the software package GSLib program SASim, while all raster-based modeling, including the addition, classification, and cross-tabulation of the individual probability surfaces, was conducted using the Idrisi software package.

2.2 Model Parameters

Parameters relating to the three main components of the simulated land-cover-change model that required specification were: 1. spatial pattern of the initial time-1 classification probability surface, 2. spatial patterns and magnitudes of the various change probability surfaces, which resulted in the time-2 classification probability surfaces, and 3. spatial patterns and magnitudes of the various error probability surfaces, which resulted in the associated time-1 and time-2 error-perturbed classification probability surfaces. The spatial pattern was controlled by the specification of a variogram model used as the primary objective function in simulated annealing, and the magnitude of the change and error surfaces was controlled by the standard deviation of the initial normal distribution.

First, to produce a classification probability surface for time-1 that exhibited a level of spatial continuity that is observable in real-world data, indicator semivariograms were fit to a forest/non-forest classification for the quarter-townships comprising Washtenaw County, Michigan. The result of variogram modeling was a distribution of semi-variogram range values, which summarized the spatial autocorrelation present in the forest/non-forest classification. Based on this distribution, a range value corresponding to the first quartile was selected and used in simulated annealing to produce a time-1 classification probability surface with a relatively low

level of spatial autocorrelation. An initial distribution of pixel values was created from $N(50, 144)$, so that the majority of classification probability values fell within one standard deviation of the classification probability cut-off. In other words, the classification probability surface for time-1 was centered at the classification probability cut-off, and the standard deviation was chosen such that almost all values fell between 0 and 100. (Note: values below 0 or above 100 were set to 0 and 100, respectively.) The size of the resulting simulated surface was chosen to approximate the average size of quarter-townships observed in Washtenaw County, Michigan.

Three different change patterns were generated to produce time-2 classification probability surfaces: 1. random, spatially auto-correlated change, 2. expansion of a single land-cover class resulting from a trend in the X direction, and 3. change that was both spatially auto-correlated and correlated to the time-1 classification boundaries. Random, but spatially auto-correlated, change probability surfaces were produced to reflect the spatial continuity of change observed in the previously-used Washtenaw County quarter-townships. Indicator variogram models were fit to binary change maps created from forest/non-forest classifications for each quarter-township and a distribution of semi-variogram range values for change was determined. Again, a single range was selected based on this distribution to summarize the spatial autocorrelation observed in the binary change maps. The value selected corresponded to the third quartile of the semi-variogram range distribution to reflect a relatively high degree of spatial continuity in change. Additionally, to produce time-2 classification probability surfaces that captured the variety of percent change observed within each quarter-township, the distribution of percent change observed between the time-1 and time-2 forest/non-forest classification was determined. The magnitude of the change probability surface was altered by varying the standard deviation of the initial distribution perturbed during simulated annealing. Two standard deviations were chosen, which resulted in change percentages roughly equal to the first and third quartiles of the percent change distribution, to reflect both low and high percentages of total change area. Simulated annealing was performed twice using the same variogram model, but two different initial normal distributions, to generate random, spatially auto-correlated change probability surfaces that exhibited relatively low and high magnitudes of change. Both normal distributions had means centered at 0 to ensure that both change types occurred in roughly equal proportions.

Conversely, the expansion of a single land-cover class by the addition of a trend in the X direction was produced without the use of simulated annealing. An initial scaled X trend, ranging from 0 to 1 in the west to east direction, was created. Then, based on the aforementioned percent change distribution, a series of trend multipliers were applied in order to produce change probability surfaces that corresponded to the percent change observed at the first and third quartiles. Two trend surfaces were produced that reflected both low and high percentages of change.

Finally, change probability surfaces correlated to time-1 classification boundaries were produced by utilizing the ability to incorporate secondary data in simulated annealing. First, a distance-to-classification-boundaries map was created by subtracting the mean of the initial normal distribution used to generate the time-1 classification probability surface from each pixel and then taking the absolute value. This created a secondary variable that captured the relative distance between an individual pixel and the nearest classification boundary. Next, simulated annealing was performed using a relatively low and high correlation value between the initial

probability distribution and the secondary data ($r = -0.3$ & $r = -0.7$, respectively), where the initial probability distribution equaled the absolute value of the normal distribution used to produce a low magnitude of change for the random change probability surface. The absolute value of this distribution and a negative correlation was chosen to both center high magnitudes of change probability near classification boundaries and to avoid centering a particular type of change near classification boundaries. Additionally, the same variogram model used to produce the random, spatially auto-correlated, change surfaces described above was also applied to the generation of correlated change surfaces. In summary, simulated annealing was performed twice using the normal distribution originally used to create maps exhibiting a low percentage of change as the primary variable and the distance-to-boundary map as the secondary variable. The results of simulated annealing were two maps each exhibiting high change probabilities near the boundaries between land-cover classes, but displaying either a relatively low or high degree of correlation to the boundaries themselves. The final step in creating the correlated change maps was to add change directionality back into the final change probability surface. To accomplish this, a binary grid comprised of 1 and -1 randomly assigned to each pixel was produced and multiplied to each simulated annealing output map. Thus, two change probability surfaces were produced, with change similar in magnitude to the low percentage change case, but with change concentrated near the classification probability boundaries at relatively low and high levels.

The final step in developing the land-cover-change simulation model involved the generation of a series of error patterns to produce both the time-1 and time-2 error-perturbed classification probability surfaces. Three different error patterns were investigated: 1. random, spatially auto-correlated error both at time-1 and time-2, 2. random, spatially auto-correlated error at time-1 with time-2 errors temporally correlated to the time-1 error pattern, and 3. errors at time-1 that were both spatially auto-correlated and correlated to time-1 classification boundaries with time-2 errors temporally correlated to the time-1 error pattern. Unlike the change probability surfaces, the variogram model used to generate error probability surfaces was not based on real-world data. This stems from the fact that comprehensive error information is often not known or available over an entire region of interest. Instead, a range value for the variogram model was chosen so that the error probability surfaces had a smaller degree of spatial autocorrelation than the change probability surfaces. The primary parameter of interest in simulating error probability surfaces was the standard deviation of the initial distribution, which controlled the overall percentage of errors in the resulting classified error-perturbed land-cover maps. A standard deviation was selected so that the misclassification rate for the error-perturbed maps was approximately 25%; i.e. a 75% overall accuracy for the land-cover map.

Random, spatially auto-correlated error probability surfaces for the time-1 and time-2 maps were generated similar to the random change probability surfaces, but a different variogram model and initial normal distribution was used in simulated annealing. Again, the normal distribution was centered at 0 to ensure that error occurring in both directions was present in roughly equal proportions. Additionally, the generation of the time-1 error probability surfaces correlated to time-1 classification boundaries also followed the same procedure as the generation of the correlated change surface, where the degree of correlation corresponded to the relatively low level ($r = -0.3$) used in change. The initial normal distribution and variogram model used to produce the correlated error surfaces corresponded to same parameters used earlier to generate the random error probability surfaces. The only new step necessary to generate error surfaces

was the creation of temporally correlated time-2 error probability surfaces. In all cases where time-2 error probability were correlated to the time-1 patterns, the resulting time-1 error probability surfaces produced through simulated annealing were used as secondary data in time-2 error surface generation. The degree of correlation to the time-1 error surfaces was defined as either 0.2 or 0.4 to reflect the range of temporal correlation values often seen in practice (Carmel, 2004). Again, the same variogram model and initial normal distribution used in the generation of the time-1 error probability surfaces was used in the generation of the time-2 temporally-correlated error probability surfaces.

2.3 An Example Model Run

The end result of a single run of the simulated land-cover-change model is the production of a single true change map that is compared to a series of error-perturbed change maps. For this research, 30 different error-perturbed probability surfaces were generated for each time-1 and time-2 map, which resulted in 30 error-perturbed change maps. Thirty was chosen so that the distribution of statistics calculated for each error-perturbed change map (i.e. PCC values) would be approximately normal, allowing for more thorough comparisons between the different change/error combinations.

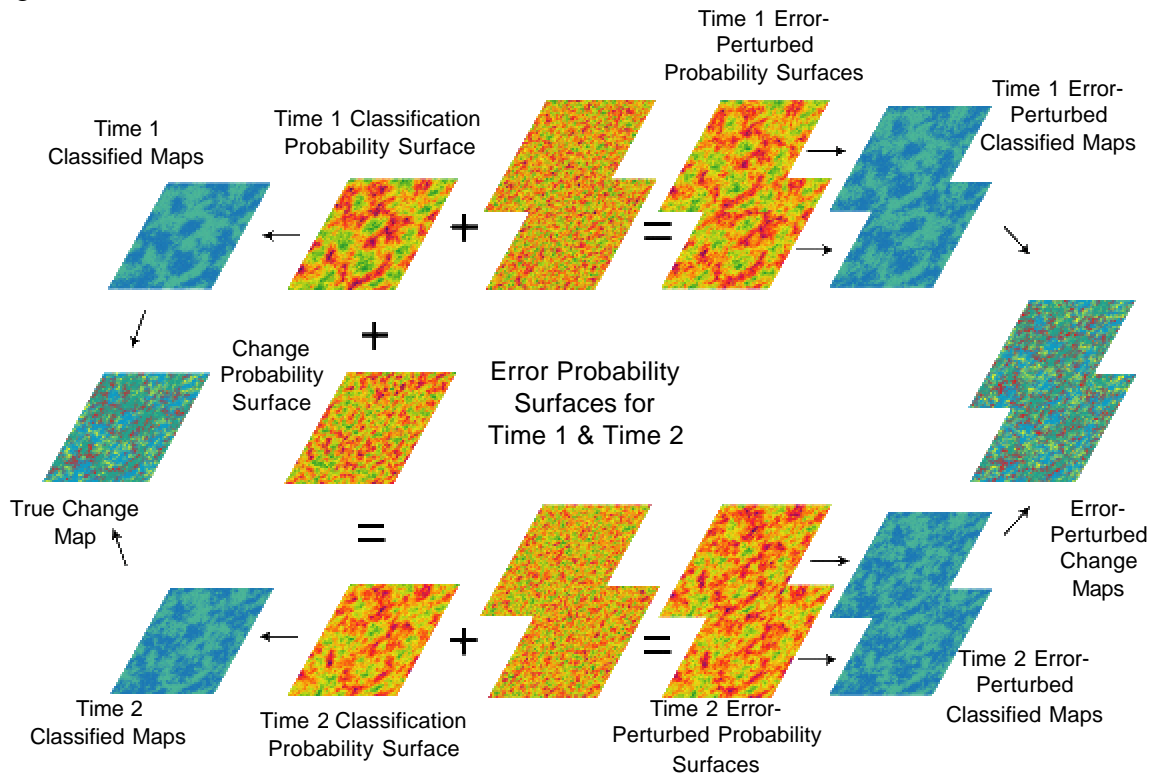


Figure 2. Diagram of an example model run illustrating the overall modeling procedure and model results.

In all, 30 different change/error combinations were modeled in this research, corresponding to the 6 possible change probability surfaces and 5 possible error probability surfaces.

3. Results

For each error-perturbed change map generated for a specific change/error combination, the overall percent correctly classified (PCC) and the user's accuracy of the two possible change categories was calculated based on the corresponding true change map. Both measures were calculated using the entire grid area. The overall PCC statistic is well known in remote-sensing research and provides a good benchmark for evaluating the impact of temporal dependencies on the accuracy of change-detection. User's accuracy for correctly predicting either change type in the error-perturbed change map was calculated because the primary interest of this research was to evaluate how well post-classification change-detection performs in predicting land-cover change in the presence of error. Separating the model's ability to predict change from its ability to predict persistence provides a better assessment of the change accuracy of the error-perturbed change map than the overall PCC value. Due to the dominance of persistence and the ease in predicting stationarity in land-cover class over time, the overall PCC value tends to be inflated in accuracy (Pontius et al, 2004). [Note: In this research, change was confined to approximately 13% -22% of the grid area depending on the low or high percentage change case.] Therefore, the user's accuracy for the combined change classes was included to assess the reliability of the land-cover transitions predicted by the error-perturbed change maps.

The resulting 30 values for both PCC and user's accuracy in predicting change were summarized by calculating the mean and standard deviation of the distribution of values. Table 1 displays the mean PCC values for the 30 possible change/error combinations, while Table 2 displays the mean user's change accuracy for the 30 possible change/error combinations.

Table 1. Mean overall percent correctly classified values with associated standard deviations for each change and error pattern combination when comparing each error-perturbed change map to its corresponding true change map for simulation modeling using 2 land-cover classes and a classification cut-off corresponding to the 50th percentile.

Change Patterns	Error Patterns				
	Random at T1 & T2	Random T1 & Temporal Correlation = 0.2 T2	Random T1 & Temporal Correlation = 0.4 T2	Low Correlation to Class Boundaries T1 & Temporal Correlation = 0.2 T2	Low Correlation to Class Boundaries T1 & Temporal Correlation = 0.4 T2
	Random with low % of change	58.889 0.004	59.283 0.004	61.127 0.005	59.651 0.003
Random with high % of change	59.949 0.004	60.629 0.004	61.247 0.006	60.318 0.003	61.042 0.003
X trend with low % of change	58.485 0.004	60.007 0.004	60.435 0.005	59.033 0.003	60.23 0.004
X trend with high % of change	59.223 0.004	59.777 0.004	60.615 0.005	59.502 0.003	60.408 0.003
Low Correlation to Class Boundaries	59.208 0.004	60.039 0.005	61.247 0.006	59.72 0.003	60.788 0.004
High Correlation to Class Boundaries	59.613 0.004	60.358 0.005	61.442 0.005	59.924 0.003	60.851 0.004

Table 2. Mean user's change accuracy with associated standard deviations for each change and error pattern combination when comparing each error-perturbed change map to its corresponding true change map for simulation modeling using 2 land-cover classes and a classification cut-off corresponding to the 50th percentile.

Change Patterns	Error Patterns				
	Random at T1 & T2	Random T1 & Temporal Correlation = 0.2 T2	Random T1 & Temporal Correlation = 0.4 T2	Low Correlation to Class Boundaries T1 & Temporal Correlation = 0.2 T2	Low Correlation to Class Boundaries T1 & Temporal Correlation = 0.4 T2
	Random with low % of change	18.819 0.003	18.605 0.003	18.560 0.003	18.467 0.003
Random with high % of change	34.027 0.003	34.344 0.004	34.709 0.006	34.064 0.003	34.696 0.004
X trend with low % of change	21.342 0.003	20.982 0.003	20.869 0.005	21.161 0.003	21.235 0.004
X trend with high % of change	28.371 0.004	28.150 0.003	28.208 0.005	28.211 0.004	28.436 0.004
Low Correlation to Class Boundaries	21.910 0.004	21.943 0.004	22.085 0.004	21.442 0.003	21.400 0.004
High Correlation to Class Boundaries	23.965 0.004	23.933 0.004	24.213 0.004	23.031 0.003	22.731 0.005

An examination of Table 1 reveals a general increasing trend in overall PCC values as the temporal correlation between the time-1 and time-2 error patterns increases. It is clear that differences exist in both the magnitude of PCC values observed and in the relative impact temporal dependencies have on the overall PCC values for the different types of change patterns. Additionally, when both change and error are correlated to classification boundaries, the overall PCC values are less than those observed when errors occur randomly throughout the grid area. Examining the standard deviations corresponding to each PCC value, it is evident that the 30 error-perturbed change maps exhibited great similarity in their overall accuracy; all standard deviations are less than 0.01. Therefore, although the relative differences between the various error patterns are small, these differences can be considered significant when incorporating the standard deviations.

An examination of Table 2 reveals much different trends in user's accuracy values for the combined change classes when considering temporal dependencies as compared to those trends observed in Table 1. First, not all change types exhibit an increase in user's change accuracy as the temporal correlation between the error patterns of time-1 and time-2 increases. In fact, a decreasing trend is observed for both random change occurring in low percentages and change resulting from a trend in the X direction when errors are random at time-1. Further, when errors at time-1 are correlated to classification boundaries, more change patterns show a decrease in their user's accuracy for the combined change classes. Second, unlike Table 1, the change patterns that consider a trend in the X direction display higher accuracies when errors are correlated to classification boundaries as compared to errors occurring randomly throughout the grid. However, some similarities to Table 1 remain. First, Table 2 supports the observation that the various change patterns respond differently to temporal dependencies, and also reveals that the user's accuracy values for the combined change classes vary greatly among the change patterns. Further, the user's accuracy values continue to exhibit decreased accuracy when both change and error are correlated to classification boundaries. Finally, the standard deviations

calculated from the distribution of user's change accuracies for each change/error combination remain small. This indicates that there continues to be great similarity between the user's change accuracy values calculated for each error-perturbed change map within a single change/error combination, and that the perceived differences between patterns can be interpreted as significant.

4. Discussion

Several outcomes can be drawn from the results presented above. First, the presence of a temporal correlation between error patterns improved the overall accuracy of the change maps. For example, looking across any row in Table 1 illustrates that as the temporal correlation between time-1 and time-2 error patterns increased from 0 to 0.2 to 0.4, the overall mean PCC values also increased significantly. Therefore, an increase in temporal correlation resulted in an increase in the overall accuracy for the error-perturbed change map. This was the case for all change patterns. However, it is interesting to note that the overall increase in accuracy differed among the various change patterns. For example, changes that were random and occurred in low percentages saw an increase in accuracy of 2.238% from no temporal correlation to a 0.4 temporal correlation, while changes that were highly correlated to classification boundaries and occurred in low percentages saw an increase of 1.829%. Thus, a second conclusion that can be drawn from Table 1 is that certain change patterns are less affected by the presence of a temporal correlation.

When comparing specific change patterns using the amount of relative change, lower levels of observed change were more affected by temporal correlations. For example, the gain in accuracy for the random change pattern with a low percent of net change was 2.238% when increasing the temporal correlation from 0 to 0.4 as compared to an increase of 1.298% for the random change pattern with a high percent of net change. This pattern also holds true for change resulting from a trend in the X direction. Therefore, as the amount of change occurring between time-1 and time-2 decreased, the presence of a temporal correlation became more important in terms of the impact it had on the overall accuracy of the change map. Additionally, cases where both the change probability surface and error probability surface were correlated to the time-1 classification boundaries showed lower overall accuracy values, even in the presence of a temporal correlation. For example, the gain in accuracy for changes that were highly correlated to classification boundaries and occurred in low percentages when errors were randomly located at time-1 and the temporal correlation was increased from 0 to 0.4 was 1.829% as compared to a gain of only 1.238% when errors were correlated to time-1 classification boundaries. As expected, both change patterns that centered high change probabilities at the classification boundaries showed lower overall accuracies than the other four change patterns when high error probabilities were also centered at classification boundaries.

Unfortunately, many of these same conclusions do not hold true when considering the results of Table 2, which illustrated how well the error-perturbed change maps performed at specifically predicting land-cover transitions. First, the presence of a temporal correlation between error patterns did not necessarily improve the accuracy of the change maps in predicting land-cover transitions. Only two of the six change patterns consistently increased in accuracy as the temporal correlation between time-1 and time-2 error patterns increased from 0 to 0.2 to 0.4 when considering random error patterns at time-1. Therefore, an increase in temporal correlation

did not correspond to a clear or significant relationship in the accuracy of predicting change for the error-perturbed change maps.

Second, while clear differences among the various change patterns were also observed when examining Table 2, the relationships and conclusions drawn from user's change accuracies were often the opposite of those drawn from overall accuracies in Table 1. For example, Table 1 showed that as the amount of change occurring between time-1 and time-2 decreased, the presence of a temporal correlation became more important in terms of the impact it had on the overall accuracy of the change map. Examining Table 2 shows that when considering error randomly located at time-1, an increase in temporal correlation has a greater impact on change patterns exhibiting a higher percentage of change. Changes that were random and occurred in low percentages saw a decrease in user's change accuracy of 0.259% from no temporal correlation to a 0.4 temporal correlation, while changes that were random and occurred in high percentages saw an increase in accuracy of 0.682%. Thus, as the amount of change occurring between time-1 and time-2 increased, the relative magnitude of the accuracy in predicting land-cover transitions was more affected by the presence of a temporal correlation. In other words, the presence of a temporal correlation between error patterns over time impacted low percent change cases more in terms of overall accuracy, but impacted high change cases more in terms of the accuracy in actually predicting change.

However, some conclusions drawn from Table 1 are also supported by the results of Table 2. First, it is clear that certain change patterns are less affected by the presence of a temporal correlation than others. Using the example illustrated previously for overall accuracies, changes that were random and occurred in low percentages saw a decrease in accuracy of 0.259% from no temporal correlation to a 0.4 temporal correlation, while changes that were highly correlated to classification boundaries and occurred in low percentages saw an increase of 0.249%. Thus, the type of change pattern considered continues to play an important role in determining the relative impact temporal dependencies have on the accuracy of predicting land-cover transitions. Second, cases where both the change probability surface and error probability surface were correlated to the time-1 classification boundaries had user's change accuracies that were smaller than those observed when errors were random at time-1. For example, the gain in accuracy for changes that were highly correlated to classification boundaries and occurred in low percentages when errors were randomly located at time-1 and the temporal correlation was increased from 0 to 0.4 was 0.175% as compared to a decrease of 0.51% when errors were correlated to time-1 classification boundaries and the temporal correlation was increased to 0.4. Again, both change patterns that centered high change probabilities at the classification boundaries saw a larger magnitude in the decrease of user's accuracy for change when high error probabilities were also centered at classification boundaries than the other four change patterns.

5. Conclusion

In summary, the above conclusions support the conjecture that different change and error patterns have significantly different effects on both the overall accuracy of the change map and the accuracy in predicting the occurrence of land-cover transitions. Further, the impact of the presence of a temporal correlation between error patterns over time differs with varying change and error patterns. However, two differing overall conclusions can be drawn from each table: 1) an increase in temporal dependence between error surfaces, regardless of whether time-1 errors

are randomly located or centered near classification boundaries, led to a significant increase in the overall accuracy of the error-perturbed change maps, and 2) an increase in temporal dependence between error surfaces, regardless of whether time-1 error are randomly located or centered near classification boundaries, did not result in a significant or predictable relationship when considering the reliability of the land-cover transitions predicted by the error-perturbed change maps. Therefore, the presence of a temporal dependence between the error patterns associated with each classified map increased the overall accuracy of the resulting change map, but did not lead to an increase in accuracy for predicting actual land-cover changes. While these conflicting results remain, this research clearly demonstrates that temporal dependencies must be considered when attempting to quantify the accuracy of land-cover-change maps. Further, the relative impact of a temporal dependence on both the overall accuracy and the accuracy in predicting land-cover transitions is dependent upon the pattern of change and pattern of error associated with a time-series of classified maps. Thus, both the presence of a temporal dependence between the errors of classified images and the pattern and magnitude of change occurring over time are critical to understanding the accuracy of a change map.

6. Acknowledgements

This research was financially supported by the Earth System Science (ESS) fellowship program funded by the National Aeronautics and Space Administration. The author also acknowledges the assistance and guidance provided by Dr. Daniel G. Brown, Associate Professor in the School of Natural Resources & Environment at the University of Michigan, and Dr. Pierre Goovaerts, Chief Scientist at BioMedware, Inc.

7. References

- Arbia, G., Griffith, D., and Haining, R., 1998, Error propagation modelling in raster GIS: overlay operation. *International Journal of Geographical Information Science*, **12**, 145-167.
- Bárdossy, A., and Samaniego, L., 2002, Fuzzy rule-based classification of remotely sensed imagery. *IEEE Transactions on Geoscience and Remote Sensing*, **40**, 362-374.
- Carmel, Y. (2004) Characterizing location and classification error patterns in time-series thematic maps. *IEEE Transactions on Geoscience and Remote Sensing*, **1**, 11-14.
- Carmel, Y., and Dean, D.J., 2004, Performance of a spatio-temporal error model for raster datasets under complex error patterns. *International Journal of Remote Sensing*, **25**, 5283-5296.
- Congalton, R.G., and Green, C., 1999. *Assessing the Accuracy of Remotely Sensed Data: Principles and Practices* (Boca Raton, Florida: CRC/Lewis Press).
- Goodchild, M.F., Guoqing, S., and Shiren, Y., 1992, Development and test of an error model for categorical data. *International Journal of Geographical Information Systems*, **6**, 87-104.
- Goovaerts, P., 1997. *Geostatistics for Natural Resource Evaluation* (New York: Oxford University Press).
- Goovaerts, P., and Journel, A.G., 1996, Accounting for local probabilities in stochastic modeling of facies data. *SPE Journal*, **1**, 21-29.
- Hogg, R.V., and Tanis, E.A., 1993. *Probability and Statistical Inference* (New York: MacMillian Publishing Co.).
- Liu, H., and Zhou, Q., 2004, Accuracy analysis of remote sensing change detection by rule-based rationality evaluation with post-classification comparison. *International Journal of Remote Sensing*, **25**, 1037-1050.

- Pontius, R.G., Shusas, E., and McEachern, M., 2004, Detecting important categorical land changes while accounting for persistence. *Agriculture, Ecosystems and Environment*, **101**, 251-268.
- Pontius, R.G., and Lippitt, C., 2004, A method to distinguish real landscape change from map error during map comparison. Conference proceedings of the joint meeting of *The Fifteenth Annual Conference of The International Environmetrics Society and The Sixth Annual Symposium on Spatial Accuracy Assessment in Natural Resources and Environmental Sciences*. (Portland ME).
- Powers, A.C., 2004, Patterns of uncertainty in land cover change analyses. Presentation at the *2004 Annual Meeting of the Association of American Geographers*. (Philadelphia, PA).